Inventory of Supplementary Materials

One supplemental table

Table S1 is related to Figure 1

Two supplemental figures

Figure S1 is related to Figure 2

Figure S2 is related to Figure 3

Eleven Supplemental Movies

Movie S1 is related to Figure 1

Movie S2 is related to Figure 2A-C

Movie S3 is related to Figure 2A-C

Movie S4 is related to Figure 2D

Movie S5 is related to Figure 2E

Movie S6 is related to Figure 3 A and B

Movie S7 is related to Figure 4A

Movie S8 is related to Figure 4A and B and Figure 4D and F

Movie S9 is related to Figure 4G and H and Figure 4I and J

One Supplementary Experimental Techniques

Supplementary Information

Supplementary Table 1.

Frequency of breaks	0.03 +/-0.01 breaks/minute/cell (n=83 cells, 1100 minutes of observation)
Frequency of strain events	0.18 +/-0.03 events/minute/cell (n=83 cells, 1100 minutes of observation)
Mean recovery rate of actin fluorescence signal	1.20 +/- 0.18 fluorescence intensity units/second (n=10)
Percent recovery	142.6 +/- 12% (n=11)
Average maximum elongation distance	2.5 +/- 0.2μm (n=10)
Elongation rate	4.0 +/- 1.4 μm/min; (n=10)
Half-time to cessation of elongation	77 +/- 6 seconds (n=10)
Strain event recovery/break	82%/18%

Figure S1:

Recovery of zyxin-GFP is rapid and not significantly different in SF and FA.

(A) Zyxin-GFP FRAP recovery t1/2 for FA (n=78) and SF (n=61) are not significantly different (P=0.3716).

(B) Example SF FRAP showing micrograph of SF with linescan of fluorescence intensity plotted below.

(C) Pooled FA and SF recovery curves.

(D) Western blot showing population levels of rescue constructs in stable cell lines.

Figure S2:

Peak traction forces are lower in zyxin (-/-) cells than zyxin (-/-) cells expressing zyxin-GFP.

(A) Color-mapped traction force images, with cell outline overlaid, showing higher peak forces in the rescued cell.

(B) Graph of binned force vector frequencies showing quartile divisions.

Supplementary Movie Legends

Movie S1:

Related to Figure 1. Spinning disk confocal time-lapse movies of two cells expressing actin-mCherry. The arrows in the first three frames indicate the location of the SF elongation and thinning event. In the movie on the left, the thinned SF recovers. In the movie on the right, the SF elongation and thinning site fails to stabilize, resulting in a catastrophic SF break. The dimensions of each movie panel are 14 x 30 μm.

Movie S2:

Related to Figure 2A-C. Multichannel spinning disk confocal time-lapse movies of a cell expressing zyxin-GFP and actin-mCherry. The arrows in the first four frames indicate the location of the SF elongation and thinning event. In the zyxin:GFP movie on the left, zyxin accumulates rapidly at the site of SF elongation. In the actin-mCherry movie on the right the SF elongates and thins locally, then recovers. The dimensions of each movie panel are 21 x 42 μm.

Movie S3:

Related to Figure 2A-C. Multichannel spinning disk confocal time-lapse movies of a cell expressing zyxin-GFP and actin-mCherry. In the actin-mCherry movie on the left, the SF

elongates and thins locally, then recovers. In the zyxin:GFP movie on the right, zyxin accumulates rapidly at the site of SF elongation. The merge panel shows zyxin in green, actin in magenta. The white box on the actin panel describes the location of details.The dimensions of each movie panel are 55 x 57 µm.

Movie S4:

Related to Figure 2D. Spinning disk confocal time-lapse movie of a zyxin-GFP expressing cell being prodded with a polished glass pipette. The arrow indicates the location of the edge of the probe. The dimensions of the movie panel are 61 X 83 µm.

Movie S5:

Related to Figure 2E. Spinning disk confocal time-lapse of a zyxin-GFP expressing cell plated on a flexible polyacrylamide substrate embedded with red fluorescent beads (red channel not shown.) The micrograph is overlaid with scaled vectors representing the magnitude of bead displacement. Vectors have been placed on a grid and do not represent the actual location of the fluorescent beads. The blue arrow represents 0.75µm of bead displacement. The white bracket highlights the SF elongation event shown in Figure 2G and analyzed in Figure 2I. The dimensions of the movie are 40 X 21µm.

Movie S6:

Related to Figure 3A and B. Spinning disk confocal time-lapse movies of a wild-type (left) and zyxin (-/-) (right) cells expressing actin-mCherry. The arrows in the first four frames indicate the location of the SF elongation and thinning event. In the wild-type cell, the site of SF elongation rapidly recovers. In the zyxin (-/-) cell the SF elongates and thins locally, then continues to extend and eventually breaks. The dimensions of each movie panel are 13 X 28 µm.

Movie S7: Related to Figure 4A. Multichannel spinning disk confocal time-lapse movies of a cell expressing zyxin-GFP. Time of saponin and Rhodamine-actin perfusion is indicated by ***. The dimensions of each movie panel are 5 X 43 μm.

Movie S8:

The left two panels are related to Figure 4A and B. Multichannel spinning disk confocal time-lapse movies of a cell expressing zyxin-GFP and α-actinin-mCherry. The arrows in the first three frames indicate the location of the SF elongation and protein accumulation. The dimensions of each movie panel are 14 X 34 μm.

The right two panels are related to Figure 4D and F. Multichannel spinning disk confocal time-lapse movies of a zyxin (-/-) cell expressing actin-mCherry and α-actinin-GFP. The arrows in the first three frames indicate the location of the SF elongation and protein accumulation. Note that α-actinin-GFP does not accumulate at the SF strain site in the zyxin (-/-) cell and the SF ultimately breaks. The dimensions of each movie panel are 16 X 35 μm.

Movie S9:

The left two panels are related to Figure 4G and H. Multichannel spinning disk confocal time-lapse movies of a cell expressing VASP-GFP and zyxin-mCherry. The arrows in the first three frames indicate the location of the SF elongation and protein accumulation. The dimensions of each movie panel are 16 X 27 μm.

The right two panels are related to Figure 4I and J. Multichannel spinning disk confocal time-lapse movies of a zyxin (-/-) cell expressing α-actinin-mCherry and VASP-GFP. The arrows in the first three frames indicate the location of the SF elongation and protein accumulation. The dimensions of each movie panel are 13 X 24 μm.

Supplemental Methods

DNA constructs

pZyx-mCherry- The mCherry coding sequence (Shaner et al., 2004) was PCR amplified to add BamHI and NotI restriction sites. The PCR products were digested in BamHI and NotI and then ligated into pEGFP-zyxin, replacing the EGFP coding sequence.

pcDNA3 α-actinin-mCherry- HindIII/XbaI EGFP fragment of pCDNA3 α-actinin: EGFP was replaced with a PCR product of mCherry with HindIII and XbaI sites. mCherry was amplified from pZyx-Cherry.

pmCherry-actin- The mCherry coding sequence was amplified from pRSET-B-mCherry, digested with AgeI and BglII and ligated in place of GFP in pEGFP-actin (Clontech, cat# PT3265-5).

pZyx4F>A Using site directed mutagenesis the phenylalanines were mutated to alanine in each of zyxin's four proline-rich (FPPP) sequences (ActA repeats). This was cloned into the pLINX viral transformation vector.

*pZyx*Δ*1-42* This N-terminal truncation of zyxin was generated using a PCR based approach, then cloned into the Tol2 Gateway transformation vector.

Other plasmids were generous gifts from; Dr. Michael Davidson (Florida State University): pActin:mApple; Dr. Frank Gertler (Massachusetts Institute of Technology): pVASP:GFP; Dr. Carol Otey (University of North Carolina, Chapel Hill): α-actinin-GFP.

Traction Microscopy

Preparation of polyacrylamide (PAA) substrates and live cell traction microscopy

Fibronectin-coated PAA substrates containing 40nm fluorescent spheres were prepared on glass coverslips (Gardel et al., 2008; Sabass et al., 2008) using a 7.5% acrylamide/0.1% bis-acrylamide gel, with a shear elastic modulus, *G'*, of 12,000 Pa. Fibronectin was covalently attached to the top surface of the PAA gel by utilizing the bifunctional cross-linker sulfo-SANPAH (Pierce).

Coverslips containing cells bound to PAA substrates were mounted in a perfusion chamber (Warner) in F12 media supplemented with 30 μL/1 mL Oxyrase (Oxyrase Enzyme system, EC0050). Cells were imaged on a spinning disk confocal microscope that consisted of a 2.5 W water-cooled Coherent Innova 70c Krypton/Argon ion laser with the 488 and 647 nm lines selected via a polychromatic acousto-optical modulator (PCAOM, Neos Technologies), Yokogawa CSU-10 scanhead mounted on a Nikon TE-2000E automated inverted microscope equipped with a Perfect Focus system (Nikon) and a linearly encoded robotic stage (Applied Scientific Instruments). Temperature control was maintained using an air curtain incubator (Nevtek). Images were generated with a 60x 1.2 NA Plan Apo water immersion objective lens (Nikon) using a 1.5X optovar. Zyxin-GFP images were captured at 10 sec intervals, and latex spheres were captured at 30 sec intervals using a Roper HQ 2 camera equipped with an interline transfer CCD (6.4 um pixel size). Following imaging, cells were perfused with 2 mL of 0.5% trypsin to release them from the PAA substrate, and an image of beads in the unstrained substrate was taken in the 647 channel.

Image Analysis

Time-lapse bead images were aligned to the reference frame with pixel accuracy, either using MetaMorph software or using custom algorithms in Matlab (Ji and Danuser, 2005). For

detection of bead displacement, a series of beads were tracked using cross-correlation tracking (Ji and Danuser, 2005). Template sizes were adaptively chosen between 11x11 and 25x25 pixels (1 pixel=0.067 mm) depending on the local image contrast. This corresponds to 1.3-3 times the diameter of a diffraction-limited image region created by the beads. Templates were placed on the positions of significant beads (Crocker and Grier, 1996). We typically obtained 1000-3000 vectors of bead displacements for each image frame of our movie.

Regions around sites of cell adhesion to the extracellular matrix were drawn based on the zyxin-GFP localization to FAs and the strain field was interpolated using a Gaussian-weighted kernel onto the centroid of the drawn region. We found this measurement to be insensitive to small variations in region geometry or location and showed similar variation as measuring the 90% of max strain within the region. The magnitude of local deformation in the compliant matrix provides a robust approximation of the magnitude and direction of the force generated by the cell at FAs.

Whole-cell traction force analysis

To isolate stress vectors within the whole cell area, a binary mask was created by thresholding intensity of zyxin-GFP or α-actinin-GFP in the zyxin (-/-) cells. Some force is propagated through the PAA gel outward from the cell edge. The whole-cell binary mask underwent circular dilation (80-pixel diameter) to extend its edge to include these force vectors. Vector magnitudes outside the cell were defined as background forces and only vectors whose magnitudes were greater than background were included in whole-cell traction force analysis.

Vector magnitude frequency from each frame was plotted on a histogram. Traction stress was binned in 50 Pascal increments on the x-axis. The frequency data was averaged using all frames and using both zyxin (-/-) cells and zyxin (-/-) +zyxin-GFP in order to find a general

distribution of quartiles. The area under the curve was found for each quartile in each frame and plotted as a single point in a scatter plot. The area underneath the curves in the fourth quartile—representing the uppermost forces exerted by a cell at one time point—was found to be significantly greater in the cells containing zyxin.

Supplemental Figure 1

Figure S1
Associated with Figure 2

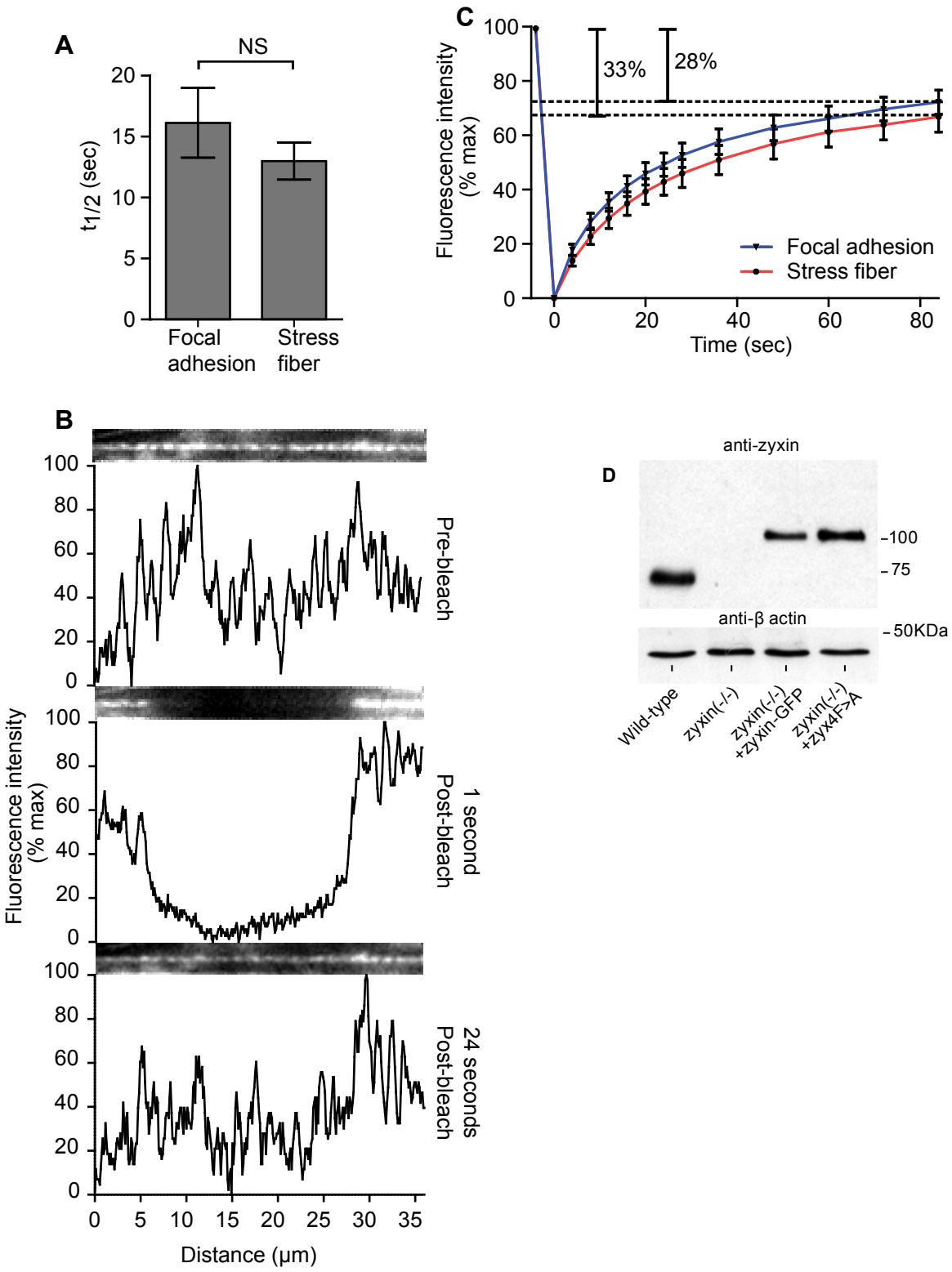

Supplemental Figure 2

Figure S2
Associated with Figure 3